Title
In situ TEM observation of FCC Ti formation at elevated temperatures

Authors
Yu, Qian
Kacher, Josh
Gammer, Christoph
et al.

Publication Date
2017-11-01

DOI
10.1016/j.scriptamat.2017.06.033

Peer reviewed

Scripta Materialia 140 (2017) 9–12

Contents lists available at ScienceDirect

Scripta Materialia

journal homepage: www.elsevier.com/locate/scriptamat

In situ TEM observation of FCC Ti formation at elevated temperatures

Qian Yu [a,b,c,*], Josh Kacher [b,c,**], Christoph Gammer [b,c,1], Rachel Traylor [b,c], Amit Samanta [d], Zhenzhong Yang [e,f], Andrew M. Minor [b,c]

[a] Center of Electron Microscopy and State Key Laboratory of Silicon Materials, Department of Materials Science and Engineering, Zhejiang University, Hangzhou 310027, People's Republic of China
[b] Department of Materials Science and Engineering, University of California, Berkeley, CA, United States
[c] National Center for Electron Microscopy, Molecular Foundry, Lawrence Berkeley National Laboratory, Berkeley, CA, United States
[d] Lawrence Livermore National Laboratory, Livermore, CA, United States
[e] Beijing National Laboratory for Condensed Matter Physics, Institute of Physics, Chinese Academy of Sciences, Beijing 100190, China
[f] Collaborative Innovation Center of Quantum Matter, Beijing 100190, China

ARTICLE INFO

Article history:
Received 20 May 2017
Received in revised form 17 June 2017
Accepted 17 June 2017
Available online 4 July 2017

Keywords:
FCC titanium
In situ TEM
Nano-mechanical testing

ABSTRACT

Pure Ti traditionally exhibits the hexagonal closed packed (HCP) crystallographic structure under ambient conditions and the body centered cubic (BCC) structure at elevated temperatures. In addition to these typical structures for Ti alloys, the presence of a face centered cubic (FCC) phase associated with thin films, interfaces, or high levels of plastic deformation has occasionally been reported. Here we show that small FCC precipitates form in freestanding thin foils during *in situ* transmission electron microscope (TEM) heating and we discuss the potential origins of the FCC phase in light of the *in situ* observations. This FCC phase was found to be stable upon cooling and under ambient conditions, which allowed us to explore its mechanical properties and stability *via* nanomechanical *in situ* TEM testing. It was found that FCC platelets within the HCP matrix phase were stable under mechanical deformation and exhibited similar mechanical deformation behavior as the parent HCP phase.

1. Introduction

Ti alloys display three different phases on the temperature/pressure phase diagram: the HCP phase (α-Ti), the BCC phase (β-Ti) and a hexagonal phase (ω-Ti). The α-phase (HCP) is the ambient-conditions stable phase. When heated to ~882 °C at atmospheric pressure it transforms to the β-phase (BCC), and transforms to the hexagonal ω-phase under high pressure conditions (2–9 GPa) [1–3]. Pure β-Ti is not stable at room temperature, unless heavily alloyed with β-stabilizers. In general, alloying leads to dramatic increases in strength at the cost of reduced ductility for both α-Ti and β-Ti alloys [4,5].

Apart from the phases seen in the equilibrium phase diagram, many studies have reported the presence of a FCC Ti phase. This phase was first reported by Wawner et al. in 1969 in single crystalline epitaxial thin films deposited on NaCl substrates of varying orientations and temperatures [6]. They reported that Ti deposits with an FCC structure and subsequently transforms to the equilibrium HCP structure at a critical thickness. This critical thickness was dependent on the substrate surface orientation and temperature, which was maximized at 500 °C on a {110} surface. These findings, as well as additional deposited thin film studies, indicate that the criteria for FCC Ti stability are related to film thickness, surface orientation, and temperature [6–11]. FCC Ti has also been widely observed in Ti-Al, -Ni, and -Ag multilayer films, where it was found that an HCP to FCC transformation occurred during cross-sectional ion-milling/thinning of the multilayer for TEM studies. Interestingly, the transformation did not occur during plan view milling for all of the Ti-multilayer studies [12–14]. However, it is unclear if this observed thinning orientation dependency was a consequence of surface orientation, beam damage induced by ion milling, or a combination of the two. Zhang and Ying observed small amounts of FCC Ti after ball milling Ti-Al powders and concluded the transformation was thermally induced, with the energy provided from the ball milling process [15]. Jing et al. observed the formation of a metastable FCC-Ti phase during heat treatment processing of a Ti-20Zr-6.5Al-4 V alloy [16]. Upon cooling from 905 °C, they detected the presence of FCC laths forming from the boundaries of α-Ti grains. After further aging at 700 °C, the FCC phase was completely replaced by α-Ti. Consequentially, it was concluded that defect accumulation and grain refinement promote the formation of the FCC phase [17,18]. Recently, Sarkar et al. reported that a FCC Ti structure formed during two different TEM sample preparation methods, ion milling and electro-polishing, within the α-phase of

* Correspondence to: Q. Yu, Center of Electron Microscopy and State Key Laboratory of Silicon Materials, Department of Materials Science and Engineering, Zhejiang University, Hangzhou 310027, People's Republic of China.
** Correspondence to: J. Kacher, School of Materials Science & Engineering, Georgia Tech, Atlanta, GA 30332, United States.
E-mail addresses: yu_qian@zju.edu.cn (Q. Yu), josh.kacher@mse.gatech.edu (J. Kacher).
[1] Present address: Erich Schmid Institute of Materials Science, Austrian Academy of Sciences, Jahnstraße 12, 8700 Leoben, Austria.

http://dx.doi.org/10.1016/j.scriptamat.2017.06.033
1359-6462/

the metastable β-Ti alloy, Ti-15 V-3Sn-3Cr-3Al [19]. It was suggested that the transformation occurred as a means to reduce the intrinsic stresses formed during alloy processing. Finally, FCC Ti has been theoretically shown to exist by Aguayo et al. using first principles calculations [20] and by Xiong et al. using a Gibb's free energy calculation [21]. Xiong et al.'s calculations showed that the FCC phase was thermodynamically stable in Ti nanoparticles with diameters below ~27 nm at elevated temperatures (~882 °C). The prevalence of this FCC phase in thin films or under high strains has been explained by the minimization of Gibb's free energy [21], stability under compressive stresses found in thin films [7], and epitaxial stabilization [6,8]. However, despite the vast number of sightings, there is little agreement on the reported FCC-Ti lattice parameters, which range from 4.02 Å [10] to 4.42 Å [22,23]. Furthermore, the driving force and mechanism behind the HCP to FCC phase transformation in Ti, as well as the mechanical stability of the FCC-Ti phase, have yet to be determined.

In the present work, we observed the thermally-induced formation of FCC-Ti in thin HCP-Ti TEM foils. It was found that the phase transformation during *in situ* TEM annealing occurred at approximately 600 °C in the thinner regions of the samples, *i.e.* near the edge of the hole in the TEM foil. To our knowledge, this is the first direct observation of a high temperature FCC Ti phase nucleation. The phase transformation is discussed in terms of potential phase transformation mechanisms and the possible role of chemistry (oxide or hydride formation).

2. Experimental methods

Ti–0.1 wt% O ingots were prepared for TEM characterization by first cutting thin sheets of material by electrodischarge machining, grinding them to approximately 100 μm thick, and punching out 3 mm disks. Final thinning to electron transparency was accomplished using a Fischione twin jet polisher with 6% perchloric, 39% butanol, and 55% methanol electrolyte maintained at a temperature of −30 °C. Sample characterization and heating was conducted in a JEOL 3010 LaB_6 TEM operated at 300 kV, a FEI TitanX operated at 300 kV, and the TEAM 0.5 microscope located at the National Center for Electron Microscopy. The TEAM 0.5 is a double-aberration-corrected STEM/TEM capable of producing images with 50 pm resolution.

In situ TEM heating and deformation experiments were conducted in the JEOL 3010 TEM. Samples were heated at a rate of approximately 1 °C/s from ambient temperature up to 900 °C in a stepwise manner, with the heat ramping paused every 50–100 °C to allow for stabilization. Nanopillar compression experiments were conducted using a Hysitron PI95 picoindenter. Square cross-section nanopillars were cut from the edge of the thinned Ti samples after *in situ* TEM annealing using focused ion beam (FIB) machining. The nanocompression tests were performed in displacement-control mode with a displacement rate of 2 nm/s. Multiple samples were prepared from a single grain to maintain the crystallographic compression direction consistent between samples.

Samples were characterized after the *in situ* annealing experiments by an array of techniques, including bright and dark field imaging (BF and DF TEM), high angle annular dark field scanning TEM (HAADF-STEM), nanobeam diffraction (semi-convergence angle of 1.5 mrad), energy dispersive X-ray spectroscopy (EDS), and electron energy loss spectroscopy (EELS).

3. Results and discussion

Pre-annealing inspection of the polished Ti samples showed that the sample was initially composed of only α-Ti. During *in situ* TEM annealing, small precipitates were observed to form. These precipitates formed only in the thin regions of the sample, *i.e.* those regions nearest the hole in the center of the TEM sample, and were not spatially correlated with any observable microstructural feature such as grain boundaries or pre-existing dislocations. An example of this behavior is shown in Fig. 1. In this case, the sample had been heated previously in the TEM to a temperature of 650 °C, resulting in the formation of larger FCC islands (indicated by an arrow in Fig. 1a). This initial formation of FCC islands occurred away from the area being irradiated by the electron beam. Upon reheating the sample, short line segments nucleated throughout the foil at a temperature of ~600 °C. The contrast was suggestive of dislocations, but this could not be confirmed due to the transient nature of the experiments. The segments had a strong directionality in their growth, apparent in Fig. 1c. Further heating led to the formation of small FCC regions located adjacent to the short segments, which, over the course of approximately 4 min, grew in size to an average projected width of 48 nm and length of 72 nm. At this point, the regions stabilized and remained stable upon cooling the sample back to ambient temperature. Diffraction patterns from before and after heating are shown in Fig. 1e. The appearance of new diffraction spots after heating were indexed and found to be consistent with a FCC crystal structure. A dark-field image using a HCP matrix diffraction condition acquired after the heating showed that the FCC phase formed with a dislocation or high strain region on one side, indicated by an arrow in the inset in Fig. 1f.

The crystal orientation relationship between FCC and HCP phases was studied post-annealing using HAADF-STEM analysis in the TEAM 0.5 microscope. Fig. 2 shows the raw HAADF-STEM image and the associated inverse fast Fourier transformation (FFT) filtered image using the FFT patterns from the HCP and FCC phases. The lattice parameter of FCC Ti was measured from the image to be $a_{FCC} = 4.12 \pm 0.03$ Å. In addition, the following orientation relationships can be identified: $(01\overline{1}1)$ ~2° (002) and $(2\overline{1}10)$ ~1° $(\overline{1}11)$. Here the angle represents the deviation from perfect alignment of the planes. These results are consistent with the basal plane in HCP-Ti aligning with a {111} plane in FCC Ti. Periodic contrast variations at the boundary are Moiré fringes associated with the boundary plane inclination with respect to the electron beam direction. Confirmation of the (0001)//{111} orientation relationship is given by the nanobeam diffraction patterns and associated STEM image shown in Fig. 2c–d. The nanobeam pattern was collected from a different sample after it was subjected to the same *in situ* TEM annealing treatment as was used to form the precipitate shown in a–b.

In order to investigate the deformation behavior of the FCC phase relative to the HCP phase, single and dual-phase nanopillars were machined from the electron transparent edge of the jet-polished disks. Understanding the mechanical properties of FCC Ti is important for the following reasons: 1) to better understand how the thermally or mechanically induced nucleation of FCC Ti might impact the mechanical properties of Ti (as seen in [15–18]), 2) to determine the mechanical stability of the FCC phase, and 3) to satisfy the scientific interest associated with understanding the properties of a new phase. As shown in the inset of Fig. 3a, single-phase FCC Ti, single-phase HCP Ti, and dual-phase HCP/FCC Ti pillars were machined. All the tested pillars had similar sizes, approximately 200 nm in diameter and 400 nm in length, and were machined from a single parent HCP grain to maintain a consistent compression direction. From the video recording of the nanocompression test (Suppl. Vid. 1–3), it can be seen that plasticity was accommodated in all samples *via* dislocation activation and propagation. As expected, dislocation activation primarily occurred at the contact surface between the indenter tip and the pillar, but quickly spread throughout the pillar interior. In the FCC pillars, this resulted in the formation of discrete slip steps on the pillar surface (Suppl. Vid. 1). Such features were not present on the deformed HCP pillars (Suppl. Vid. 2). In the dual-phase pillar, the top HCP phase deformed homogeneously *via* dislocation activity during the initial stages of plastic deformation. The deformation then quickly transferred to the interior FCC phase where a large number of pre-existing dislocations were activated (Suppl. Vid. 3). No significant dislocation activity was observed in the lower HCP phase even after significant deformation in the top HCP and FCC phases had occurred. Furthermore, no dislocation transfer across the HCP/FCC phase boundary and no apparent boundary instabilities, such as boundary sliding, was observed.

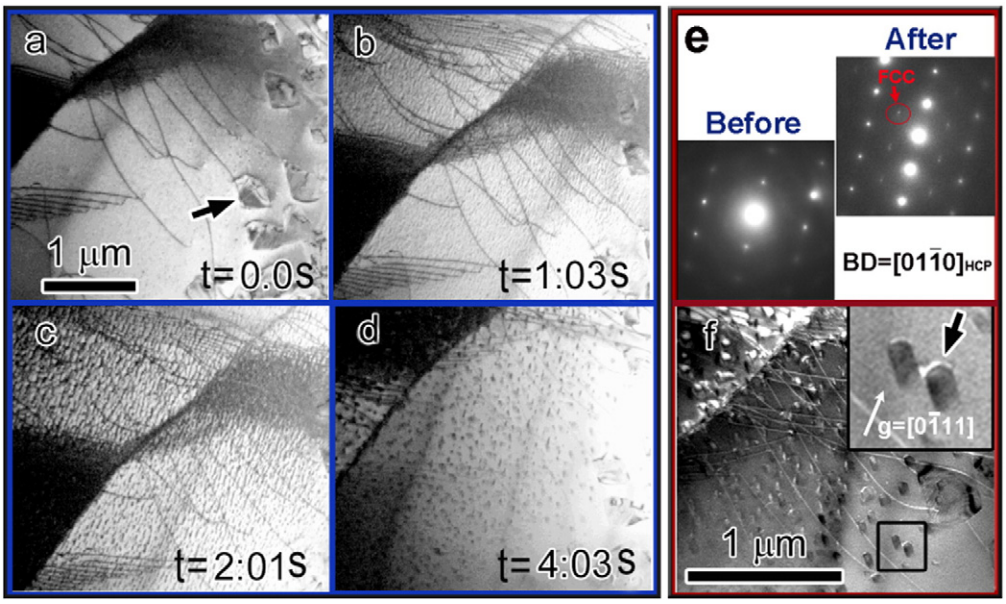

Fig. 1. a, b, c, and d are BF TEM images captured from the *in situ* TEM heating experiment showing the formation and growth of the new phase from HCP matrix (Suppl. Vid. 4). The beam direction is $[01\bar{1}0]_{HCP}$. e) Diffraction patterns from the *in situ* heating experiment showing the appearance of new FCC spots after formation of the FCC platelets. f) DF TEM image showing the short dislocation segments or strain localization at the phase boundary (indicated by arrow in inset).

The representative engineering stress-displacement curves of FCC, HCP and HCP/FCC two-phase pillars are plotted in Fig. 3. All three systems had similar yield strengths, approximately 1.75 GPa, and exhibited ductile deformation up to the maximum applied strain (approximately 0.3 for all three pillars). The maximum stress in compression was calculated by using the maximum load and the real time contact surface area. The maximum stress achieved in the two-phase samples was also much higher than the than those computed from either of the single-phase HCP and FCC pillars, reflective of the increased work hardening rate associated with the phase boundary. As the mechanical behavior of the two phases are similar, these results suggest that the FCC Ti regions reported by other groups after thermal and mechanical processing [15–18] should have similar influence on the mechanical behavior as grain refinement of the HCP phase, though it is difficult to draw broad conclusions from limited testing.

The experimental results above show that freestanding HCP Ti thin films can transform to an FCC structure *via* a thermally induced phase transformation. Once formed, The FCC phase remains stable, even at ambient temperatures and under compressive loads.

Previous studies have discussed the possibility of forming a FCC-Ti phase in terms of free energy minimization [21,23], where surface energies and interfacial constraints are considered to be the important factors. The restriction of phase nucleation to the thinnest regions of the specimens as seen in this study is consistent with this concept. The observed orientation relationships also agree with what was theoretically demonstrated by Bauer et al. for allotropic HCP-FCC phase transformations in Co [24]. Their mechanism relies on gliding partial dislocations transforming a HCP ABAB stacking sequence to a FCC ABCAB stacking sequence. If the partial dislocations reside on every other close-packed plane, so-called 'ordered glide', the HCP matrix is transformed allotropically to FCC. As the close-packed plane for HCP materials is the basal plane, this mechanism should result in an (0001)//{111} orientation relationship, which is in agreement with Fig. 2. Interestingly, in the results reported here, the FCC phase did not revert to HCP upon cooling. This may be due to FCC being stabilized by the free surfaces in the thin foil.

The effect of impurities also must be taken into account when considering the origin of the FCC phase transition. Variants of Ti hydrides

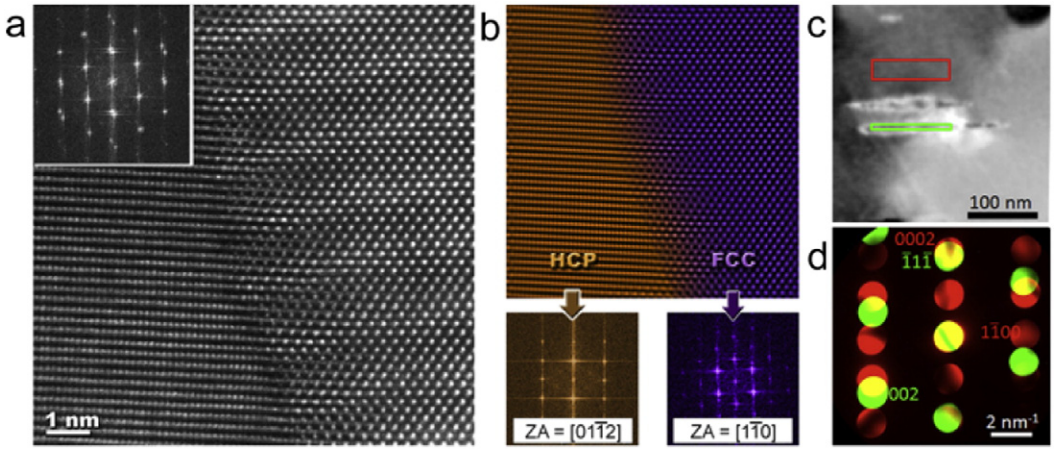

Fig. 2. a) HAADF-STEM image of HCP and FCC Ti interface. b) Colorized image using the inverse of the FFT patterns of HCP and FCC phases from (a). c) DF STEM image of two FCC precipitates. d) Nanobeam diffraction patterns collected from FCC region (green) and HCP matrix (red). Colors correspond to boxed regions in panel c.

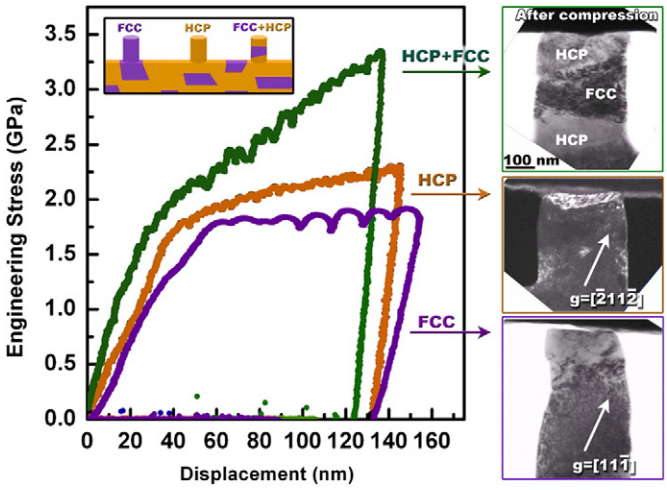

Fig. 3. The engineering stress-displacement curves of nanocompression tests on an HCP + FCC pillar, an HCP pillar and a FCC pillar, respectively. The TEM images of those pillars after deformation are also shown. Videos of the deformation behavior can be seen in Suppl. Vid. 1–3.

have often been suggested as the culprit for the observed FCC Ti phase in the literature [25]. Only the Ti-δ hydride ($TiH_{1.5-2}$) demonstrates an FCC-like structure, *i.e.* Ti-δ has the CaF_2 prototype phase structure where Ti atoms occupy FCC sites, while Ti-γ and Ti-ε hydrides have face-centered tetragonal (FCT) structures with c/a ratios of 1.09 and 0.96 respectively [26]. However, the possibility that the observed FCC-Ti phase is a type of Ti-hydride can quickly be ruled out as Ti-hydrides are known to be unstable at temperatures above 300 °C, *i.e.* the (α + β) eutectoid temperature in the Ti-H binary phase diagram [25]. Ti also forms FCC-like impurity compounds with oxygen (γ-TiO), nitrogen (TiN), and carbon (TiC), all with NaCl type structures. Of these, γ-TiO is the most likely as it is stable at elevated temperatures and, due to the native oxide existing on the polished foil surfaces and the imperfect vacuum conditions of the electron microscope, there are potential sources of O for the transformation. EDS and EELS measurements of the precipitates did not conclusively show any O enrichment relative to the levels in the surrounding matrix, though it is difficult to analyze this effect with such small precipitates surrounded by an inevitable native oxide. The mechanical testing results are also suggestive that the FCC phase is not an oxide as it is unlikely that an oxide would have similar mechanical properties as the native HCP phase. Atom probe tomography could potentially provide a definitive answer, but such an investigation is outside the scope of the present study.

To summarize, it was observed that a thermally-induced HCP to FCC phase transformation occurs in Ti thin films at a temperature of approximately 600 °C. The FCC phase was shown to remain stable upon cooling to ambient temperatures and displayed considerable dislocation-based plasticity under nanocompression tests. EDS and EELS analysis did not show any O enrichment in the particles themselves, though additional characterization is needed to definitively rule out oxidization effects.

Supplementary data to this article can be found online at http://dx.doi.org/10.1016/j.scriptamat.2017.06.033.

Acknowledgements

We gratefully acknowledge funding from the US Office of Naval Research under Grant No. N00014-12-1-0413. C.G. acknowledges support by the Austrian Science Fund (FWF):[J3397]. The work by A.S. was performed under the auspices of the U.S. Department of Energy by Lawrence Livermore National Laboratory under Contract DE-AC52-07NA27344. Work at the Molecular Foundry was supported by the Office of Science, Office of Basic Energy Sciences, of the U.S. Department of Energy under Contract No. DE-AC02-05CH11231. Q.Y. acknowledges support by the Chinese 1000-Youth-Talent Plan, 111 project under Grant No.·B16042, National Natural Science Foundation of China (51671168) and the State Key Program for Basic Research in China under Grant No. 2015CB65930. We acknowledge Mark Asta, Max Poschmann and Daryl Chrzan for useful discussion in the preparation of this manuscript.

References

[1] W. Petry, A. Heiming, J. Trampenau, M. Alba, C. Herzig, H.R. Schober, G. Vogl, Phys. Rev. B 43 (13) (1991) 10933–10947.
[2] D.A. Young, Phase Diagrams of the Elements, Universit of California Press, Berkeley, CA, 1991.
[3] J.C. Jamieson, Science 140 (3562) (1963) 72–73.
[4] G. Lutjering, J.C. Williams, Titanium, 2nd ed Springer, Heidelberg, 2007.
[5] D. Banerjee, J.C. Williams, Acta Mater. 61 (3) (2013) 844–879.
[6] F.E. Wawner Jr., K.R. Lawless, J. Vac. Sci. Technol. 6 (4) (1969) 588–590.
[7] J. Chakraborty, K. Kumar, R. Ranjan, S.G. Chowdhury, S.R. Singh, Acta Mater. 59 (7) (2011) 2615–2623.
[8] S.K. Kim, F. Jona, P.M. Marcus, J. Phys. Condens. Matter 8 (1) (1996) 25–36.
[9] Y. Yamada, K. Yoshida, Appl. Surf. Sci. 33 (1988) 465–471.
[10] L.P. Yue, W.G. Yao, Z.Z. Qi, Y.Z. He, Nanostruct. Mater. 4 (4) (1994) 451–456.
[11] M. Fazio, D. Vega, A. Kleiman, D. Colombo, L.M. Franco Arias, A. Márquez, Thin Solid Films 593 (2015) 110–115.
[12] A.F. Jankowski, M.A. Wall, J. Mater. Res. 9 (1) (1994) 31–38.
[13] D. Josell, D. Shechtman, D. van Heerden, Mater. Lett. 22 (5) (1995) 275–279.
[14] R. Ahuja, H.L. Fraser, J. Electron. Mater. 23 (10) (1994) 1027–1034.
[15] D.L. Zhang, D.Y. Ying, Mater. Lett. 50 (2–3) (2001) 149–153.
[16] R. Jing, C.Y. Liu, M.Z. Ma, R.P. Liu, J. Alloys Compd. 552 (2013) 202–207.
[17] P. Chatterjee, S.P. Sen Gupta, Appl. Surf. Sci. 182 (3–4) (2001) 372–376.
[18] I. Manna, P.P. Chattopadhyay, P. Nandi, F. Banhart, H.-J. Fecht, J. Appl. Phys. 93 (3) (2003) 1520–1524.
[19] R. Sarkar, P. Ghosal, K.S. Prasad, T.K. Nandy, K.K. Ray, Philos. Mag. Lett. 94 (5) (2014) 311–318.
[20] A. Aguayo, G. Murrieta, R. de Coss, Phys. Rev. B 65 (2002).
[21] S. Xiong, W. Qi, B. Huang, M. Wang, Z. Li, S. Liang, J. Phys. Chem. C 116 (1) (2011) 237–241.
[22] D. Shechtman, D. van Heerden, D. Josell, Mater. Lett. 20 (5–6) (1994) 329–334.
[23] D. Van Heerden, D. Josell, D. Shechtman, Acta Mater. 44 (1) (1996) 297–306.
[24] R. Bauer, E.A. Jägle, W. Baumann, E.J. Mittemeijer, Philos. Mag. 91 (3) (2011) 437–457.
[25] D. Banerjee, C.G. Shelton, B. Ralph, J.C. Williams, Acta Metall. 36 (1) (1988) 125–141.
[26] S. Banerjee, P. Mukhopadhyay, Phase Transformation: Examples from Titanium and Zirconium Alloys, Elsevier, LTD, Amsterdam, The Netherlands, 2007.